HHS Public Access

Author manuscript

J Cereb Blood Flow Metab. Author manuscript; available in PMC 2017 January 23.

Published in final edited form as:

J Cereb Blood Flow Metab. 2008 May ; 28(5): 882–886. doi:10.1038/sj.jcbfm.9600598.

Verification of enhancement of the CSF space, not parenchyma, in acute stroke patients with early blood–brain barrier disruption

Erica C Henning, **Lawrence L Latour**, and **Steven Warach**

Section on Stroke Diagnostics and Therapeutics, Stroke Branch, National Institute of Neurological Disorders and Stroke, National Institutes of Health, Bethesda, Maryland, USA

Abstract

Enhancement on post-contrast fluid-attenuated inversion recovery (FLAIR) images after acute stroke has been attributed to early blood–brain barrier disruption. Using an estimate of parenchymal volume fraction and the apparent diffusion coefficient (ADC), we investigated the relative contributions of cerebral spinal fluid (CSF) and parenchyma to enhancement seen on postcontrast FLAIR. Enhancing regions were found to have low parenchymal volume fractions and high ADC values, approaching that of pure CSF. These findings suggest that contrast enhancement on FLAIR occurs predominately in the CSF space, not parenchyma.

Keywords

ADC; blood–brain barrier; CSF; FLAIR; HARM; stroke

Introduction

After the development of intravenously administered contrast agents such as Gd-DTPA (gadolinium-diuethylene triamine penta-acetic acid), T_1-weighted contrast-enhanced magnetic resonance imaging has been employed for the assessment of blood–brain barrier (BBB) integrity in experimental (Dijkhuizen *et al*, 2001; Kastrup *et al*, 1999; Runge *et al*, 1994) and clinical stroke (Elster and Moody, 1990; Koenigsberg *et al*, 1999; Merten *et al*, 1999). Gd-DTPA does not readily cross an intact BBB; thus, the presence of image enhancement post-contrast enables the identification of BBB disruption. Recent studies have shown similar findings on T_2-weighted fluid-attenuated inversion recovery (FLAIR) imaging (Dechambre *et al*, 2000; Latour *et al*, 2004; Mathews *et al*, 1999; Warach and Latour, 2004). In both cases, the T_1 values in regions of BBB disruption are shortened from intravascular leakage of Gd contrast into the extracellular space. Because the inversion time in FLAIR imaging is selected to null the cerebral spinal fluid (CSF) signal, a shortening of the T_1 value

Correspondence: Dr EC Henning, Section on Stroke Diagnostics and Therapeutics, Stroke Branch, National Institute of Neurological Disorders and Stroke, National Institutes of Health, Building 10, Room B1D733, 10 Center Drive, MSC 1063, Bethesda, MD 20892, USA. henninge@ninds.nih.gov.

Part of this work was presented at the 15th annual meeting of the International Society of Magnetic Resonance in Medicine, Berlin, Germany, 2007.

Disclosure/Conflict of Interest

The authors have reported no conflict of interest.

because of contrast agent leakage results in incomplete suppression and marked hyperintensity.

While BBB disruption is detectable using either method, it has been suggested that T_2-weighted FLAIR imaging is more sensitive than T_1-weighted imaging to lower concentrations of gadolinium (Mamourian *et al*, 2000; Mathews *et al*, 1999). Although hyperacute lesions are generally inconspicuous on FLAIR, it is important to note that lesions at subacute or chronic time points may be hyperintense before gadolinium administration, based on the development of vasogenic edema. In contrast, the CSF, meninges, and subdural or subarachnoid space remain dark owing to the FLAIR method and suppression of the CSF signal. These regions only appear hyperintense after administration of Gd contrast (Dechambre *et al*, 2000; Latour *et al*, 2004; Mathews *et al*, 1999; Warach and Latour, 2004). Because early BBB disruption has been strongly associated with reperfusion, hemorrhagic transformation, and poor prognosis in acute stroke patients, this phenomenon has been termed HARM (Hyperintense Acute injuRy Marker) (Warach and Latour, 2004).

Although past studies have suggested that the location of HARM is in the CSF (Dechambre *et al*, 2000; Koenigsberg *et al*, 1999; Latour *et al*, 2004; Warach and Latour, 2004), the verification of CSF-based HARM versus involvement of the parenchymal space has yet to be performed. Accurate differentiation between CSF and parenchyma is needed to assess the relative contributions of each population to the HARM enhancement. Unfortunately, fast imaging techniques such as echo planar imaging (EPI) have limited spatial resolution with considerable volume averaging of gray matter, white matter, vasculature, and CSF. Because CSF is characterized by long T_2 and high apparent diffusion coefficient (ADC) values relative to gray matter and white matter, any partial volume averaging of CSF common to DW-EPI acquisition schemes will undoubtedly yield artificially high T_2 and ADC values, respectively, in human brain (Falconer and Narayana, 1997). Diffusion measurements in combination with the FLAIR technique permit a way of addressing partial volume averaging at the borders between the ventricular space, parenchyma, and sulci.

The effects of partial volume averaging of CSF and parenchyma on ADC values have been studied by combining the FLAIR preparation with DW-EPI (Bykowski *et al*, 2004). The $b = 0$ image in the FLAIR-DWI sequence is T_2-weighted with CSF suppression (i.e., FLAIR). The $b = 0$ image in standard DWI is T_2-weighted and lacks CSF suppression (i.e., T_2). Because both sequences are resolution-matched, taking the ratio of the two $b = 0$ images (FLAIR and T_2) provides an estimate of the volume fraction of parenchyma (λ_{app-p}) (Latour and Warach, 2002). ADC values, in combination with λ_{app-p} values, should permit a quantitative comparison between ischemic lesion, healthy tissue, and regions with HARM on FLAIR. We hypothesize that the HARM regions will include those areas with high ADCs and low apparent volume fractions (i.e., CSF) in contrast to normal tissue.

Materials and methods

Patient Selection and Imaging Criteria

A retrospective analysis of 10 acute stroke patients (subpopulation of previous study; Latour *et al*, 2004) was performed using the following inclusion criteria: (1) imaging performed

pre- and post-Gd contrast (FLAIR, standard DWI, FLAIR-DWI) within a 24-h time period, (2) evidence of HARM on FLAIR post-Gd contrast, and (3) observation of focal post-Gd contrast enhancement within the vascular territory of the acute stroke. Patients (five men; five women) had a median baseline NIHSS (The National Institutes of Health Stroke Scale) of 9 with an average age of 79 years. Four of ten patients received intravenous rtPA after the pre-Gd scan. Patients were imaged using a GE 1.5 T clinical MR system using the following parameters: matrix size = 128 × 128 (zero-filled to 256 × 256); 24-cm field of view (0.94 mm in-plane resolution); 20, 7-mm-thick axial-oblique slices (interleaved acquisition). Typical sequence parameters were as follows: FLAIR: TR/TE ~ 9,000/85 ms, TI ~ 1,750 ms; standard DWI: TR/TE ~ 6,000/72 ms, $b = 0$, 1,000 s/mm^2; FLAIR-DWI: TR/TE ~ 9,000/72 ms, TI ~ 2,200 ms, $b = 0$, 1,000 s/mm^2. Median scan times from symptom onset were 2 and 6 h for the pre- and post-Gd contrast imaging protocols, respectively.

Data Analysis

Image analysis and parameter map production were performed using routines written in IDL (Research Systems Inc., Boulder, CO, USA) and MIPAV (BIRSS, NIH, Bethesda, MD, USA). After midsagittal alignment, image coregistration was performed using an optimized automatic registration algorithm with six degrees of freedom, trilinear interpolation, and the normalized mutual information cost function. After coregistration of all images, ADC parameter maps were calculated based on $b = 0$ and isotropic ($b = 1{,}000$) DW images for both FLAIR-DWI and standard DWI:

$$\mathrm{ADC}=\ln\left(\frac{\mathrm{S}_0}{\mathrm{S}_{\mathrm{ISO}}}\right);\mathrm{S}_{\mathrm{ISO}}=\sqrt[3]{\mathrm{S}_\mathrm{x}\mathrm{S}_\mathrm{y}\mathrm{S}_\mathrm{z}} \quad (1)$$

where S_0 is the signal intensity in the $b = 0$ image and S_{ISO} is the signal intensity in the isotropic ($b = 1{,}000$) image. For S_{ISO}, S_x, S_y, and S_z refer to the signal intensities in $b = 1{,}000$ images acquired for each of the three orthogonal directions (x, y, z). Parameter maps for the apparent volume fraction of parenchyma ($\lambda_{\mathrm{app-p}}$) were calculated based on the ratio of FLAIR to T_2 images at baseline

$$\lambda_{\mathrm{app-p}}\frac{\mathrm{FLAIR}-\mathrm{DWI}(b=0)}{\text{standard DWI}(b=0)}=\frac{\mathrm{FLAIR}}{T_2} \quad (2)$$

Regions with HARM on FLAIR were segmented based on positive signal enhancement seen post-contrast when compared with the pre-contrast images. Additional volumes of interest were drawn for ischemic lesion and the comparable contralateral region based on isotropic ($b = 1{,}000$) DW images. FLAIR signal differences pre-versus post-Gd contrast were calculated, with normalization to the baseline (pre-contrast) signal: signal

$$\mathrm{signal}(\%\ \text{of baseline})=\frac{\mathrm{FLAIR}_{\mathrm{pre}}-\mathrm{FLAIR}_{\mathrm{post}}}{\mathrm{FLAIR}_{\mathrm{pre}}} \quad (3)$$

Scatter plots of standard ADC versus λ_{app-p} were created for individual regions (HARM, lesion, healthy tissue). The values are expressed as mean (s.d.). Two-tailed paired *t*-tests assuming unequal variances were performed to assess differences between individual regions. A value of $P < 0.01$ was considered significant.

Results

Figure 1 shows evidence of HARM for a representative acute stroke patient with early BBB disruption. Enhancement on FLAIR was never seen before Gd contrast (Figure 1, top left). After contrast administration, HARM was visible on FLAIR (Figure 1, top middle). Representative volumes of interest for HARM regions (yellow), lesion (red), and healthy tissue (blue) are shown (Figure 1, bottom right). These volumes of interest were employed for the calculation of FLAIR signal enhancement, standard ADCs, FLAIR-ADCs, and λ_{app-p} values (equations (1) to (3)).

Figure 2 (top) displays the degree of signal enhancement, expressed as percent of baseline, for HARM (yellow), ischemic lesion (red), and healthy tissue (blue). HARM regions had a significant signal increase after Gd contrast (1.81 (0.32), $P < 0.01$). There were no appreciable changes in signal for ischemic stroke (1.13 (0.09), $P = 0.21$) or healthy tissue (1.01 (0.11), $P = 0.92$). Figure 2 (bottom) displays the relationship between standard ADC values (non-CSF suppressed) and λ_{app-p} values for HARM (dot), ischemic lesion (square), and healthy tissue (plus). HARM regions had relatively low λ_{app-p} values in comparison with both ischemic stroke and healthy tissue. HARM regions had significantly higher ADCs (1.6×10^{-3} mm^2/sec (0.4)) than both ischemic stroke (0.73×10^{-3} mm^2/sec (0.08), $P < 0.01$) and healthy tissue (0.9×10^{-3} mm^2/sec (0.2), $P < 0.01$), consistent with that of CSF. Although ADCs in regions with HARM were slightly reduced from standard values for pure CSF (~ 3.0×10^{-3} mm^2/sec), partial volume averaging of CSF and normal parenchyma is likely. λ_{app-p} values for HARM regions, ischemic stroke, and healthy tissue were 0.40 (0.10), 0.74 (0.07), and 0.76 (0.08), respectively. After volume fraction correction, ADCs in HARM regions were 2.7×10^{-3} mm^2/sec (0.5). After CSF suppression, the ADCs for ischemic stroke and healthy tissue were 0.63×10^{-3} mm^2/sec (0.06) and 0.79×10^{-3} mm^2/sec (0.06), consistent with previous reports (Bykowski *et al*, 2004; Falconer and Narayana, 1997; Latour and Warach, 2002).

Discussion

After stroke, there is a delayed loss of BBB integrity within and along the lesion periphery (Kastrup *et al*, 1999). Early reperfusion may temporarily alleviate these BBB alterations, but if delayed, reperfusion will likely exacerbate the amount of endothelial injury (Huang *et al*, 1999; Kastrup *et al*, 1999; Nagahiro *et al*, 1994). BBB disruption is coupled to the inflammatory response and activation of matrix metalloproteinases (Rosell *et al*, 2006; Rosenberg *et al*, 1998). Depending on the severity and duration of insult, irreversible endothelial dysfunction may occur (Romanic *et al*, 1998). Subacute or chronic formation of edema may then lead to diapedesis of blood and hemorrhagic transformation (Dijkhuizen *et al*, 2001; Montaner *et al*, 2001). No longer considered a static entity, the BBB has become

increasingly important in its role in delayed neuroinflammation and has warranted further study.

BBB assessment has generally been performed by T_1-weighted contrast-enhanced magnetic resonance imaging. When utilizing the standard dose of Gd-DPTA (0.1 mmol/kg), T_1-weighted images have three times lower contrast-to-noise than that of FLAIR images (Mamourian *et al*, 2000; Mathews *et al*, 1999). Runge *et al* (1994) reported that T_1-weighted magnetic resonance imaging detection of BBB disruption was visible in only three of six cats at the standard dose (~25% signal enhancement), but in all six at the triple dose (100% signal enhancement) of contrast agent. These *in vitro* phantom and *in vivo* experiments indicate that CSF changes evident on FLAIR may not be evident on T_1-weighted studies.

In our study, we utilized the FLAIR technique in combination with standard DWI methods to assess the regional distribution of early BBB disruption in acute stroke patients. Hyperintensity on follow-up FLAIR often occurs because of the natural progression of the ischemic lesion and is difficult to differentiate from contrast enhancement of the CSF. Our approach to differentiate parenchymal injury from post-Gd enhancement was to estimate the volume fraction of parenchyma (λ_{app-p}) and the ADC (equations (1) and (2)) in regions that appear hyperintense on follow-up FLAIR. We found that regions with diffuse HARM were characterized by high ADCs and low λ_{app-p} values. These findings show the inclusion of the CSF space and exclusion of the parenchyma. Although we cannot conclude that Gd contrast is responsible for 100% of the enhancement seen, previous work has shown that enhancement on FLAIR never occurs before administering contrast agent. Quantitative measurements of T_1 would provide a definitive verification of contribution of Gd to CSF signal enhancement. This has not been possible to date given the logistic challenges in an acute stroke setting. Further work will be necessary to determine the exact relationship between Gd enhancement, T_1 change, and severity of BBB disruption.

Delivery of Gd contrast into the CSF/subarachnoid space may occur (1) via the ependymal barriers in periventricular regions such as the choroid plexus and leptomeninges (Ennis and Keep, 2006; Nagahiro *et al*, 1994) and/or (2) via faulty tight junctions between adjacent vascular endothelial cells (Romanic *et al*, 1998). These potential mechanisms of entry have been investigated in experimental models of stroke, but their verification in the clinical setting has yet to be performed. Because our evaluation was performed acutely, this does not rule out the involvement of the parenchyma at subacute or chronic time points. Delayed involvement of the parenchyma is likely. For these reasons, the spatiotemporal evolution of HARM on FLAIR will depend on the dose and administration of Gd contrast, as well as the timing of imaging pre- versus post-contrast.

In conclusion, early HARM occurs predominantly in the CSF space than in parenchyma. Because HARM has negative implications to patient outcome, further study of the extent of HARM severity will be useful for refinement of clinical trials and patient management. We hypothesize that the dual acquisition of standard DWI and FLAIR-DWI, when combined with the apparent volume fraction of parenchyma (λ_{app-p}), will lead to more accurate assessment of HARM severity in clinical studies of stroke progression.

Acknowledgments

The authors would like to acknowledge the clinicians of the National Institutes of Health Stroke Team at Suburban Hospital for their assistance in patient recruitment and data collection. This research was supported by the Division of Intramural Research of the National Institute of Neurological Disorders and Stroke, National Institutes of Health.

References

Bykowski JL, Latour LL, Warach S. More accurate identification of reversible ischemic injury in human stroke by cerebrospinal fluid suppressed diffusion-weighted imaging. Stroke. 2004; 35:1100–1106. [PubMed: 15060314]

Dechambre SD, Duprez T, Grandin CB, Lecouvet FE, Peeters A, Cosnard G. High signal in cerebrospinal fluid mimicking subarachnoid haemorrhage on FLAIR following acute stroke and intravenous contrast medium. Neuroradiology. 2000; 42:608–611. [PubMed: 10997567]

Dijkhuizen RM, Asahi M, Wu O, Rosen BR, Lo EH. Delayed rt-PA treatment in a rat embolic stroke model: diagnosis and prognosis of ischemic injury and hemorrhagic transformation with magnetic resonance imaging. J Cereb Blood Flow Metab. 2001; 21:964–971. [PubMed: 11487732]

Elster AD, Moody DM. Early cerebral infarction: gadopentetate dimeglumine enhancement. Radiology. 1990; 177:627–632. [PubMed: 2243961]

Ennis SR, Keep RF. The effects of cerebral ischemia on the rat choroid plexus. J Cereb Blood Flow Metab. 2006; 26:675–683. [PubMed: 16136054]

Falconer JC, Narayana PA. Cerebrospinal fluid-suppressed high-resolution diffusion imaging of human brain. Magn Reson Med. 1997; 37:119–123. [PubMed: 8978640]

Huang ZG, Xue D, Preston E, Karbalai H, Buchan AM. Biphasic opening of the blood–brain barrier following transient focal ischemia: effects of hypothermia. Can J Neurol Sci. 1999; 26:298–304. [PubMed: 10563216]

Kastrup A, Engelhorn T, Beaulieu C, de Crespigny A, Moseley ME. Dynamics of cerebral injury, perfusion, and blood–brain barrier changes after temporary and permanent middle cerebral artery occlusion in the rat. J Neurol Sci. 1999; 166:91–99. [PubMed: 10475101]

Koenigsberg RA, Gul N, Faro S, Elfont R, Baker K, Tsai F. Hyperacute cerebral enhancement: the earliest predictor of hemorrhage by MR imaging? J Neuroimaging. 1999; 9:235–236. [PubMed: 10540604]

Latour LL, Kang DW, Ezzeddine MA, Chalela JA, Warach S. Early blood–brain barrier disruption in human focal brain ischemia. Ann Neurol. 2004; 56:468–477. [PubMed: 15389899]

Latour LL, Warach S. Cerebral spinal fluid contamination of the measurement of the apparent diffusion coefficient of water in acute stroke. Magn Reson Med. 2002; 48:478–486. [PubMed: 12210912]

Mamourian AC, Hoopes PJ, Lewis LD. Visualization of intravenously administered contrast material in the CSF on fluid-attenuated inversion-recovery MR images: an in vitro and animal-model investigation. AJNR Am J Neuroradiol. 2000; 21:105–111. [PubMed: 10669233]

Mathews VP, Caldemeyer KS, Lowe MJ, Greenspan SL, Weber DM, Ulmer JL. Brain: gadolinium-enhanced fast fluid-attenuated inversion-recovery MR imaging. Radiology. 1999; 211:257–263. [PubMed: 10189481]

Merten CL, Knitelius HO, Assheuer J, Bergmann-Kurz B, Hedde JP, Bewermeyer H. MRI of acute cerebral infarcts, increased contrast enhancement with continuous infusion of gadolinium. Neuroradiology. 1999; 41:242–248. [PubMed: 10344507]

Montaner J, Alvarez-Sabin J, Molina CA, Angles A, Abilleira S, Arenillas J, Monasterio J. Matrix metalloproteinase expression is related to hemorrhagic transformation after cardioembolic stroke. Stroke. 2001; 32:2762–2767. [PubMed: 11739970]

Nagahiro S, Goto S, Korematsu K, Sumi M, Takahashi M, Ushio Y. Disruption of the blood–cerebrospinal fluid barrier by transient cerebral ischemia. Brain Res. 1994; 633:305–311. [PubMed: 8137165]

Romanic AM, White RF, Arleth AJ, Ohlstein EH, Barone FC. Matrix metalloproteinase expression increases after cerebral focal ischemia in rats: inhibition of matrix metalloproteinase-9 reduces infarct size. Stroke. 1998; 29:1020–10230. [PubMed: 9596253]

Rosell A, Ortega-Aznar A, Alvarez-Sabin J, Fernandez-Cadenas I, Ribo M, Molina CA, Lo EH, Montaner J. Increased brain expression of matrix metalloproteinase-9 after ischemic and hemorrhagic human stroke. Stroke. 2006; 37:1399–1406. [PubMed: 16690896]

Rosenberg GA, Estrada EY, Dencoff JE. Matrix metalloproteinases and TIMPs are associated with blood–brain barrier opening after reperfusion in rat brain. Stroke. 1998; 29:2189–2195. [PubMed: 9756602]

Runge VM, Kirsch JE, Wells JW, Dunworth JN, Woolfolk CE. Visualization of blood–brain barrier disruption on MR images of cats with acute cerebral infarction: value of administering a high dose of contrast material. AJR Am J Roentgenol. 1994; 162:431–435. [PubMed: 8310940]

Warach S, Latour LL. Evidence of reperfusion injury, exacerbated by thrombolytic therapy, in human focal brain ischemia using a novel imaging marker of early blood–brain barrier disruption. Stroke. 2004; 35:2659–2661. [PubMed: 15472105]

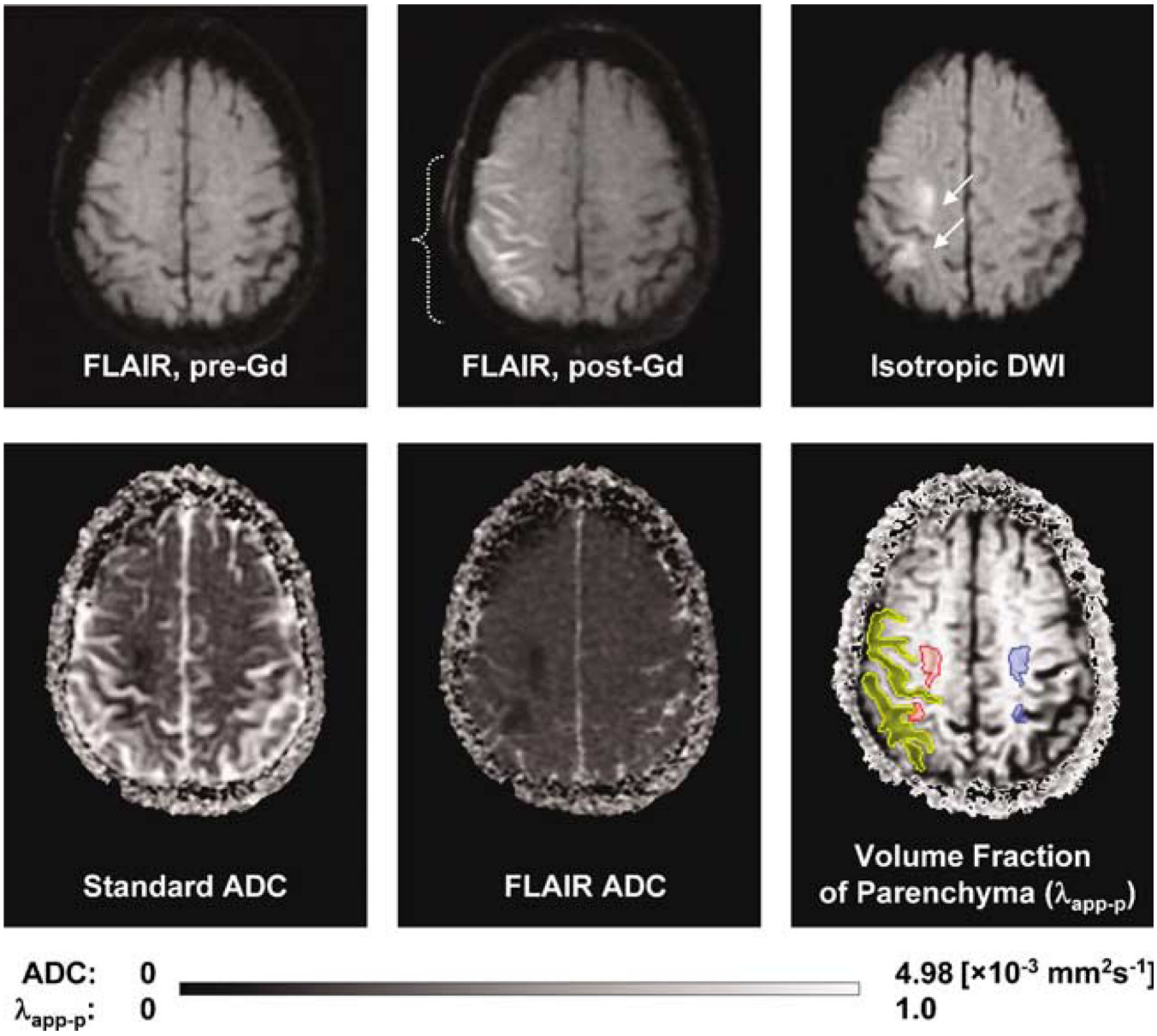

Figure 1.

Evidence of HARM for a representative acute stroke patient with early blood–brain barrier (BBB) disruption (woman, 81 years old, baseline NIHSS 17, no tPA). Top (left to right): FLAIR pre-Gd contrast, FLAIR post-Gd contrast, isotropic DWI ($b = 1000$). Bottom (left to right): standard ADC, FLAIR ADC, and volume fraction of parenchyma (λ_{app-p}) parameter maps. FLAIR enhancement was never seen before Gd contrast. After Gd contrast, FLAIR images were positive for HARM. Volumes of interest were drawn for regions with HARM (post-Gd FLAIR, brackets), ischemic lesion (isotropic DWI, arrows) and the comparable contralateral region. Scan times from symptom onset were 2 h 35 mins and 6 h 27 mins for the pre-Gd versus post-Gd contrast administration, respectively.

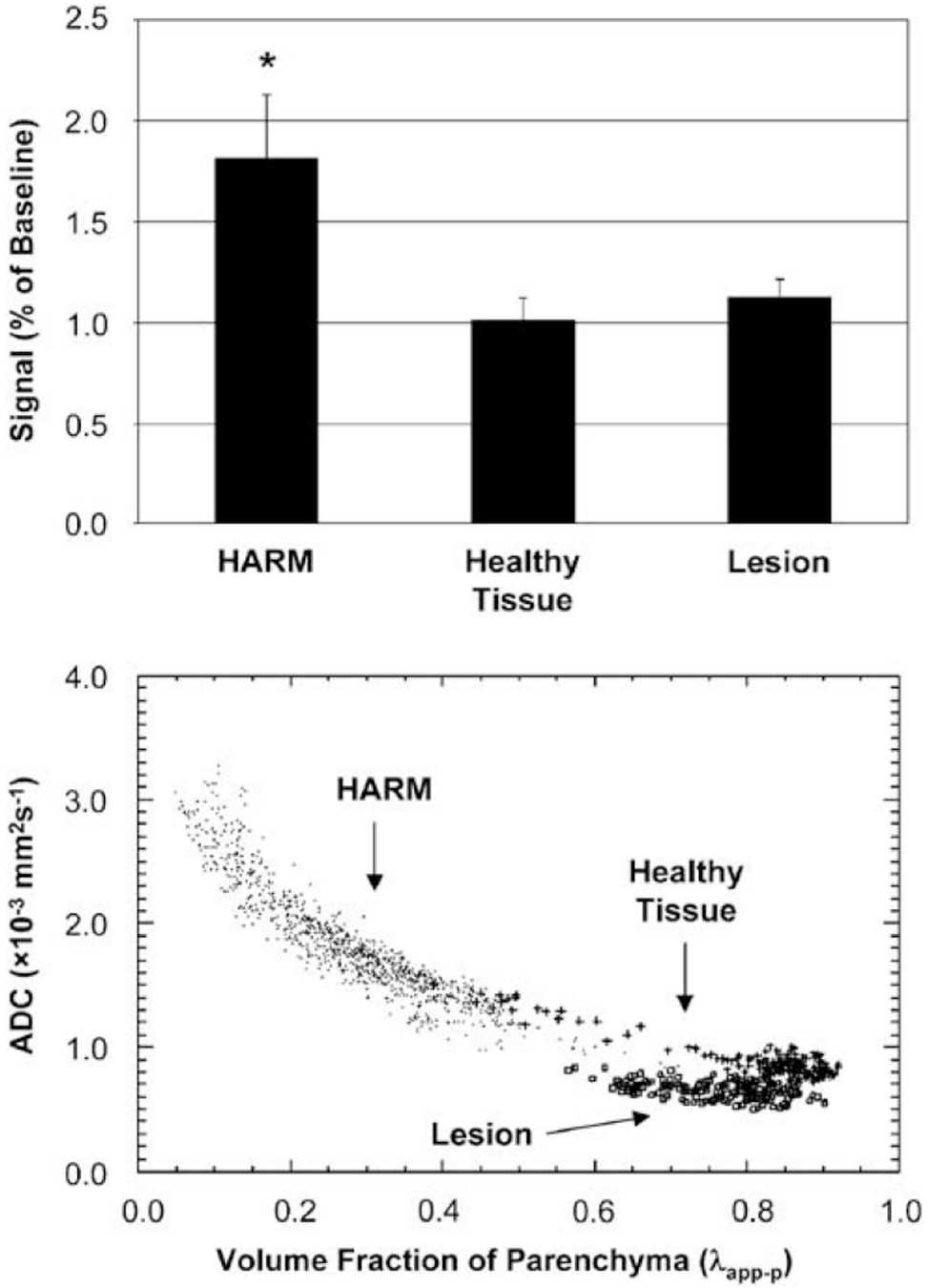

Figure 2.

Top: FLAIR signal enhancement pre- versus post-Gd contrast. HARM regions had a significant signal increase, whereas ischemic lesion and healthy tissue did not. Bottom: scatterplot of standard ADCs versus volume fraction of parenchyma (λ_{app-p}) for HARM (dot), ischemic lesion (square), and contralateral tissue (plus). Note that HARM regions have a low λ_{app-p} and high ADCs compared with ischemic stroke and normal tissue. Significance with $P < 0.01$.